

## Cationic dye adsorptions by eggshell waste: kinetics, isotherms and thermodynamics studies

Abimbola A. Ogundiran<sup>a,\*</sup>, Edwin A. Ofudje<sup>b</sup>, Olusegun O. Ogundiran<sup>c</sup>,  
Adewunmi M. Adewusi<sup>a</sup>

<sup>a</sup>Department of Chemical Sciences, Tai Solarin University of Education, Ijagun, Ogun-State, Nigeria, Tel.: +234 7066709187; emails: ogundiranaa@tasued.edu.ng (A.A. Ogundiran), whunmi09@gmail.com (A.M. Adewusi)

<sup>b</sup>Department of Chemical Sciences, Mountain Top University, Ibafo, Ogun State, Nigeria, email: eaofudje@mtu.edu.ng

<sup>c</sup>Department of Chemistry, Tai Solarin College of Education, Omu, Ogun State, email: olusegunogundiran1@gmail.com

Received 29 June 2022; Accepted 23 October 2022

### ABSTRACT

This study investigated the potential of eggshell powder (EGP) on the removal of two important cationic dyes namely: Methylene Blue (MB) and Crystal Violet (CV), by batch adsorption experiments. Characterization of eggshell functional groups was investigated using Fourier-transform infrared spectroscopy (FT-IR), scanning electron microscope (SEM) and X-ray diffraction (XRD). The experiments were carried out by varying the adsorbent dosage, pH, contact time, temperature and initial dye concentrations. The study showed that all parameters affected the removal of the dyes by the adsorbent. Pseudo-second-order kinetics model best represented the experimental data for EGP-MB, while pseudo-first-order best explained EGP-CV system. The Langmuir, Freundlich, Temkin and Dubinin–Radushkevich isotherm models were used to describe the adsorption process and of all these isotherm models, the Langmuir model best represented both adsorbate–adsorbent systems (EGP-MB and EGP-CV) giving maximum adsorption capacities ( $Q_{\max}$ ) of 122.510 and 118.610 mg g<sup>-1</sup> respectively at 35°C. Thermodynamics studies showed that both adsorption systems are spontaneous and endothermic.

*Keywords:* Methylene blue; Crystal violet; Adsorption; Eggshell

### 1. Introduction

Dyes are mainly used in textile, food, pharmaceutical and other chemical industries. Wastewater containing dyes are highly colored and noticeable even at a low concentration with large volume of synthetic dyes being disposed into the environment and water bodies [1,2].

When dye is present in water bodies at high concentrations, the reoxygenation potential of the receiving water and sunlight penetration will be limited, and biological activity in aquatic systems are also disrupted [3,4]. Synthetic dyes have carcinogenic and mutagenic properties; they remain persistent in the environment and are resistant

to biodegradation [2,3]. Their presence results in environmental pollution and health problems such as asthma, dermatitis, skin inflammation and sometimes their effect could be deadly [1,5,6]. Methylene blue (MB) (3,7-bis(dimethylamino)-phenothiazin-5-ium chloride) is a commonly used cationic dye that is highly soluble in water at room temperature [7,8]. It is extensively used to dye textiles, such as cotton, cellulose, wood, and silk [9]. It is harmful to human health above a certain concentration due to its strong toxicity, predominantly to the central nervous system [10]. Crystal violet (CV) on the other hand is popularly known as gentian violet, is a triarylmethane dye. The dye is used as

\* Corresponding author.

an antiseptic medically especially on Gram-positive organisms. Burns, boils, carbuncles, and other skin infections are treated with CV [9,11]. Since these dyes are not environmentally friendly, there is therefore an urgent need for the decontamination of these pollutants from the environment.

Among all the common techniques for residual dye removal from waste and industrial effluent such as biological treatment, coagulation, flocculation, ion exchange, membrane filtration and advanced oxidation processes [9–14], adsorption is considered and proven to be suitable for the removal of dyes from wastewater. Adsorption as a remediation technique is viable because of its ease of operation, flexibility, adaptability, simplicity of design, cost-effectiveness, efficiency, efficacy, insensitivity to toxic pollutants and eco-friendliness [15–17] and adsorbent/adsorbent regeneration [18]. In adsorption process, the widely used adsorbent is activated carbon; however, its high cost of production and level of purity has limited its application. There is therefore the urge for cheaper and effective adsorbents which can readily be deployed in dye remediation. Several adsorbents such as natural clay mineral [9], surfactant-modified laterite [13], adsorbent-ultrasonic spray [14], magnetite/pectin NPs [19], magnetite/silica/pectin NPs [19], N-benzyl-O-carboxymethyl chitosan magnetic nanoparticles [20], polymer-modified magnetic nanoparticles [21], coal [22], and anionic surfactant with silica [23] have all been documented for their ability to remove MB and CV dyes from aqueous solution.

In this work, we prepared low-cost adsorbents from waste eggshell and applied it for the removal of MB and CV dyes. Chicken eggshell is waste from homes and poultry farms which can cause nuisance to the environment and its presence could cause diseases because of its high organic matter which could harbor fungi and bacteria when disposed indiscriminately. Thus, processes like this where waste chicken eggshell can be utilized to prepare adsorbent which could be deployed in dye wastewater treatment would prove useful and the utilization of waste resources could as well be achieved as a means of environmental sustainability. Thus, the application of waste chicken eggshell in wastewater treatment is not only seen as an adsorbent but also a way of adding values to the waste product. Thus, experiments were performed to evaluate the impact of contact time, initial dye concentrations, eggshell dosage, temperature, and pH solution on the uptake of MB and CV dyes in a batch process from aqueous solution. Different kinetics and isotherm models were deployed to further provide lucid understanding about the adsorption data. Fourier transform infrared spectroscopy (FT-IR), X-ray diffraction (XRD) and scanning electron microscope (SEM) were used for the structural investigation of the adsorbent.

## 2. Materials and methods

### 2.1. Materials

Methylene Blue (MB, chemical formula –  $C_{16}H_{18}ClN_3S_2H_2O$ , molecular weight: 355.5 g/mol, 98% dye content). Crystal violet (CV, chemical formula –  $C_{25}H_{30}ClN_3$ , molecular weight: 407.99 g/mol, 98% dye content) and other reagents were purchased from Zayo-Sigma Chemicals Ltd,

Jos, Nigeria and were used without further purification. All reagents used were of analytical grade.

### 2.2. Preparation of the adsorbate solutions

A suitable quantity of MB and CV were added to deionized water to prepare a stock solution of 1,000 mg L<sup>-1</sup> respectively in a 1,000 mL volumetric flask. The standard series solutions were prepared from the previously prepared stock solution by using the dilution method. UV-VIS spectrometer (Hitachi, U3210, Japan) was used to measure the concentrations of MB and CV dyes. The absorbances were measured at  $\lambda_{max}$  664 and 590 nm for MB and CV, respectively. The pH values of the prepared MB dye solution were measured by using a pH meter of pH 21 Hanna instrument.

### 2.3. Preparation of adsorbent

Eggshell waste was collected from a cafeteria at Ijebu Ode. Eggshell collected was washed under tap water to remove dirt and dust. After that, eggshells were washed with hot water to remove stubborn dirt and then with distilled water and dried at 105°C in an oven to remove the moisture. The dried eggshell was crushed into smaller sizes using a mortar and pestle after which it was pulverized into powder and sieved through 60 mesh to obtain fine homogeneous particle size. Finally, the eggshell powder was taken as the adsorbent without any treatment.

### 2.4. Adsorbent characterization

The adsorbent surface functional groups present were investigated using FT-IR, XRD and SEM before being used and after the adsorption process. The FT-IR spectrum of eggshell was recorded using the KBr disc method at room temperature in the wavenumber range 400–4,000 cm<sup>-1</sup>. XRD were done using PANalytical (X'Pert Pro, the Netherlands) coupled with Cu K $\alpha$  ( $\gamma = 1.54178 \text{ \AA}$ ) radiation at room temperature and the peaks obtained were matched with standard files. Surface morphology characterization was done by SEM using a Hitachi (Japan) S-3000H electron microscope which contain an accelerating voltage of 15 kV. The surface charge of the biomass (also known as zero point charge) was performed using 0.2 g of the adsorbent in 20 mL of the dye solution. The pH solution was adjusted with either 0.1 M HCl or NaOH and measurements done with Zetasizer Nano ZS instrument (Malvern, UK) for the analysis of the zeta potential of the adsorbent.

### 2.5. Batch experimental studies

The experiments were carried out in Erlenmeyer flasks (100 mL) containing 10 mL of the desired concentration of dyes and the required amount of the adsorbent. The flasks were shaken for pre-determined time and speed using an orbital shaker, at 35°C unless otherwise indicated. The factors affecting the adsorption process such as contact time (0–160 min), initial dyes concentration (100–500 mg/L), adsorbent dosage (5–25 mg/10 mL), solution temperature (25°C–45°C) and initial solution pH (2.0–8.0) were investigated for both MB and CV dyes. The dye solutions' initial

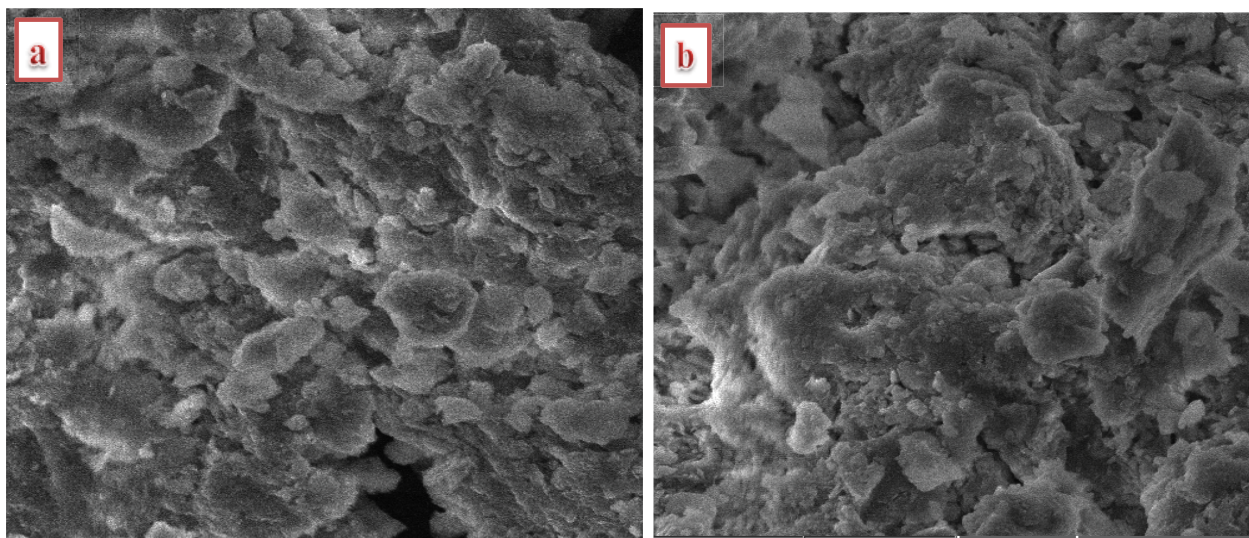


Fig. 1. SEM images of eggshell (a) before and (b) after adsorption of the pollutant.

pH was adjusted to the desired value using a solution of either NaOH or HCl (0.1 M). The experiments were conducted in triplicate. After each adsorption experiment, the adsorbent was separated by centrifugation at 2,500 rpm for 5 min. A UV-Vis spectrophotometer (Hitachi, U3210, Japan) at a maximum wavelength ( $\lambda_{\max}$ ) of 662 nm for MB and 590 nm CV respectively was used to estimate the initial and residual MB and CV concentrations. The percentage removal of the dyes (%R) and amount ( $q_e$ ) of dye adsorbed were estimated using Eqs. (1) and (2):

$$\%R = \frac{C_0 - C_t}{C_0} \times 100 \quad (1)$$

$$\text{Adsorption capacity at equilibrium, } q_e = \frac{V(C_0 - C_e)}{m} \quad (2)$$

where  $V$  (L),  $C_e$  (mg/L),  $C_0$  (mg/L),  $C_t$  (mg/L) and  $C_e$  (mg) represent volume of dye solution, concentrations at equilibrium, the initial concentration and the final concentrations at any time  $t$  and at equilibrium of MB and CV dye solutions respectively.

## 2.6. Kinetics and equilibrium studies

Kinetic studies are required in order to determine the various mechanisms which governed the adsorption process. The kinetic of the dye adsorption on eggshell was investigated and interpreted by applying the pseudo-first-order (PFO) [Eq. (3)], pseudo-second-order (PSO) [Eq. (4)], Elovich [Eq. (5)] and intraparticle diffusion [Eq. (6)] kinetic models [2,4,5,24]:

$$Q_t = Q_e(1 - e^{-k_1 t}) \quad (3)$$

$$Q_t = \frac{k_2 Q_e^2 t}{1 + k_2 Q_e t} \quad (4)$$

$$q_t = \frac{1}{\beta} (\ln \alpha \beta) + \left( \frac{1}{\beta} \right) \ln t \quad (5)$$

$$Q_t = K_{id} t^{0.5} + C_i \quad (6)$$

where  $k_1$  ( $\text{min}^{-1}$ ) and  $Q_e$  (mg/g) represent the PFO kinetic model rate constant and the calculated adsorbent capacity,  $k_2$  (g/mg min) denotes the PSO kinetic model rate constant. The Elovich rates of adsorption and desorption can be represented as  $\alpha$  and  $\beta$  in mg/g min, respectively. Whereas,  $K_{id}$  denotes the intraparticle diffusion rate constant in  $\text{mg/g min}^{0.5}$  and  $C_i$  stands for the intercept and measures the surface thickness of the adsorbent. The plots of  $Q_t$  vs.  $t$  were used to estimate all the constants using scientist software.

## 2.7. Test of kinetic fitness

The comparison between the PFO and PSO were examined via the sum of error squares (SSE, %) [4,5]:

$$\%SSE = \sqrt{\frac{\left( \left( \frac{Q_{(\text{exp})} - Q_{(\text{Cal})}}{Q_{\text{exp}}} \right) \right)^2}{N - 1}} \times 100 \quad (7)$$

The data point's number is given as  $N$ .

The equilibrium isotherm data were designed using the Langmuir, Freundlich, Temkin and Dubinin-Radushkevich (D-R) isotherm models.

From the Langmuir, the non-linear form is given as [6,15]:

$$Q_e = \frac{Q_0 b C_e}{1 + b C_e} \quad (8)$$

where  $Q_{\max}$  (mg/g) represent the maximum adsorbed amount of MB and CV respectively and  $b$  is the Langmuir isotherm model constant.

For the Freundlich isotherm, the non-linear form is expressed as [2]:

$$Q_{eq} = K_F C_e^{1/n} \quad (9)$$

where  $K_F$  stands for the Freundlich constant ( $\text{mg/g (L/mg)}^{1/n}$ ),  $n$  denotes the Freundlich intensity which is dimensionless and account for the magnitude of heterogeneity on the adsorbent surface.

The Temkin's expression is given as [5,24,25]:

$$Q_e = \frac{RT}{b_T} \ln a_T C_e \quad (10)$$

with  $R$  standing for the universal constant ( $8.314 \text{ J/mol K}$ ),  $b$  denotes Temkin's constant, and  $T$  is absolute temperature in K.

The D-R expression is given as [24,25]:

$$Q_e = Q_m e^{-\beta e^2} \quad (11)$$

Details about the parameters in the equation are described by Ofudje et al. [4] and Adeogun et al. [25]. The mean free energy of adsorption per mole of the adsorbate can be obtained from the relation:

$$E = (2\beta)^{-0.5} \quad (12)$$

If  $E$  is in the range of 8 to 16 kJ/mol, the process is chemisorption, while value of  $E$  below 8 kJ/mol depicts physical adsorption process [4].

### 3. Results and discussion

#### 3.1. Characterization of the eggshell

SEM was performed to examine the morphology of the waste eggshell before and after the adsorption of pollutant as depicted in Fig. 1a and b. Natural waste eggshell exhibited irregular structures. After the adsorption process, not

much difference was observed as shown in Fig. 1b. The waste eggshell's XRD pattern fits well with Joint Committee on Powder Diffraction Society (JCPDS) standard data of Aragonite (JCPDS no. 411475) which is an indication that the waste biomass is made up of crystalline structure of aragonite ( $\text{CaCO}_3$ ) system as depicts in Fig. 2. Important peaks corresponding to aragonite crystalline structure were deduced. However, after the adsorption of organic pollutant, shift in peak positions coupled with decrease in intensity were observed and this confirm the adsorption of the pollutant onto the surface of the biomass [4].

FT-IR investigations of the waste biomass before and after organic pollutant adsorption as presented in Fig. 3 shows that the eggshell consisted mainly of carbonate functional groups of  $\text{CaCO}_3$ . The absorption bands noticed at  $1,435$ ;  $1,125$ ;  $884$  and  $715 \text{ cm}^{-1}$  are the main component of the eggshell ( $\text{CaCO}_3$ ). The broad band noticed between  $3,498$  to  $3,663 \text{ cm}^{-1}$  are attributed to hydroxyl stretching which could be ascribe to humidity absorption [26]. Peaks noticed at  $1,120$  and  $1,457 \text{ cm}^{-1}$  were assigned to C–O bond. Nevertheless, most of the peaks in the raw biomass before adsorption process were observed to have shifted to  $1,125$ ;  $1,488$ ;  $3,562$  and  $3,669 \text{ cm}^{-1}$  after the adsorption of the pollutant. These changes are indications of interaction between the sorption groups available on the surface of the eggshells and the pollutants, thus implying electrostatic adsorption mechanism.

#### 3.2. Effects of initial dye concentration and contact time

The result of the interactions between initial dye concentrations and contact time on adsorption of MB and CV by the eggshell are shown in Figs. 4 and 5, respectively. From these plots, it was observed that the adsorption of the dye increases with the increase in the contact time to some extent and beyond this, increasing the contact time further does not increase the dye uptake process due to deposit of dyes on the available binding sites of the adsorbent material [4,5]. The dye uptake was rapid at the initial process until it reached equilibrium at a contact time of 120 min for MB and 100 min for CV respectively. It was equally established from these plots that the amount of dye

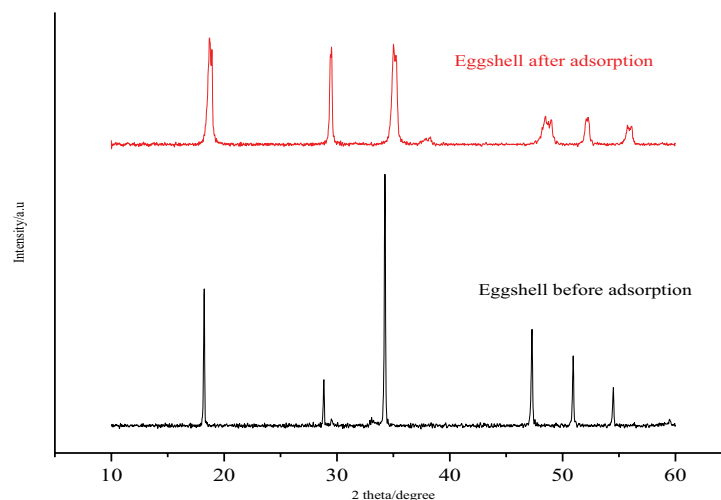


Fig. 2. XRD pattern of eggshell before and after the adsorption of the pollutant.

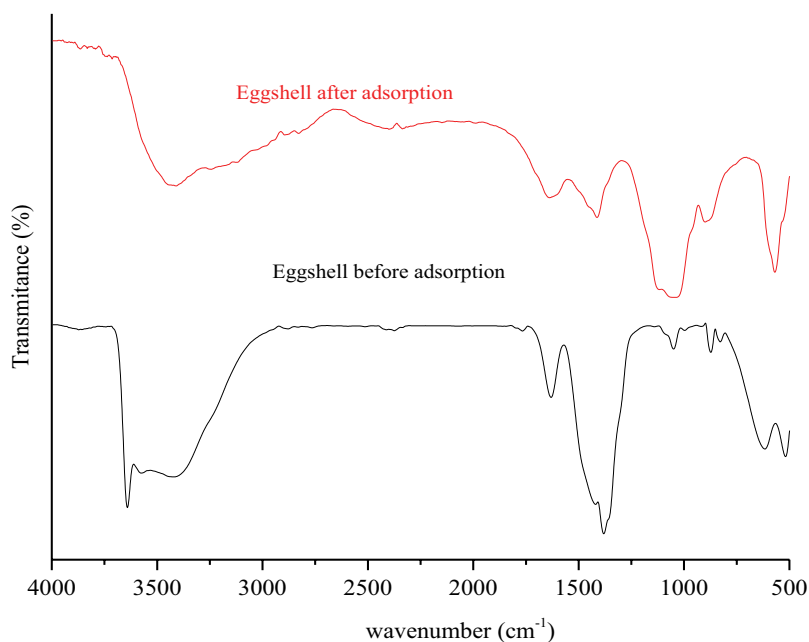


Fig. 3. FT-IR analysis of eggshell before and after the adsorption of pollutant.

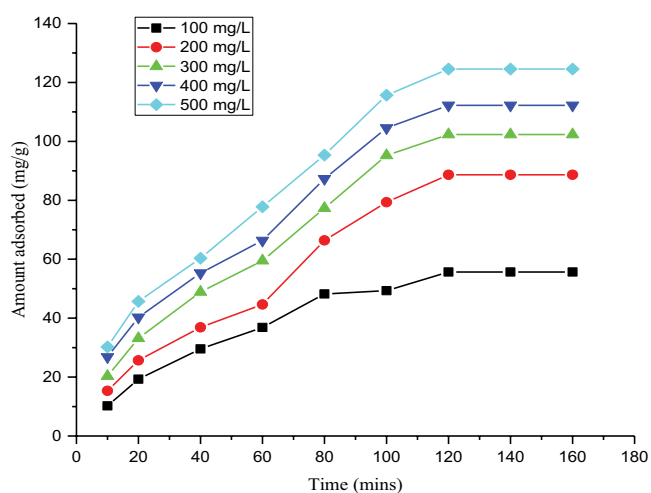


Fig. 4. Effect of initial MB concentration and contact time on the removal of MB at adsorbent: 15 mg, temperature: 35°C and pH: 5.0.

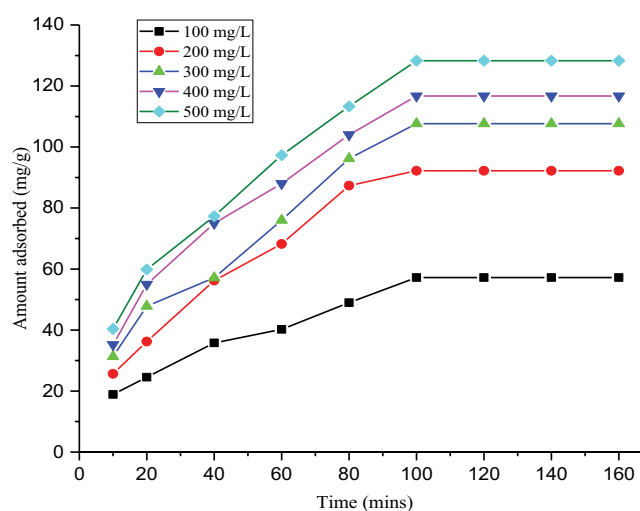


Fig. 5. Effect of initial CV concentration and contact time on the removal of CV MB at adsorbent: 15 mg, temperature: 35°C and pH: 5.0.

uptake increased as the concentrations of the dye increases which is due to the enhancement of driving force available in the aqueous solution which enables the dye particles to diffuse faster onto the surface of the adsorbent [4].

### 3.3. Effect of pH on the adsorption of the dyes

In adsorption process, pH is an important parameter due to its effect on the charge on the adsorbent surface and ionization of its molecules. Over the range of pH 2.0–8.0, the effect of pH of dye solution on the adsorption was studied. A plot of percent removal against pH is presented in Fig. 6 and it shows that the percentage removal of both dyes

increased as the pH increases from 2.0–5.0 with optimum adsorption pH of 5.0 for both dyes. Maximum percentage removal of 78.4% and 73.2% were achieved for CV and MB at pH 5.0. The  $pH_{ZPC}$  of the biomass obtained 4.2 and above this value, the surface of the eggshell is expected to be negatively charged. Since the two dyes are cationic species, this will enhance their adsorption onto the negatively charged surface of the biomass and this explains the reason why the adsorption of the dyes was favored at a pH 5.0 [5]. However, at basic pH, the anionic forms of the dyes dominate the medium with excess of hydroxyl groups which causes precipitation of the solution and thereby causing reduction the uptake process. The surface of the eggshell is

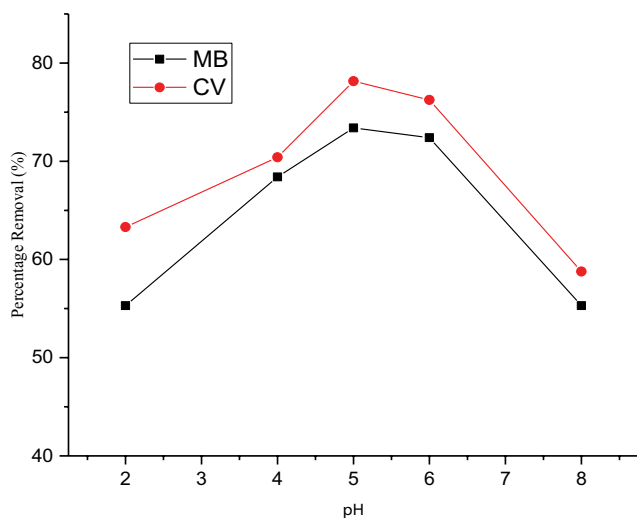


Fig. 6. Effect of pH on the adsorption process at adsorbent: 15 mg, initial pollutant concentration of 500 mg/L, temperature: 35°C, time of 100 and 120 min for MB and CV, respectively.

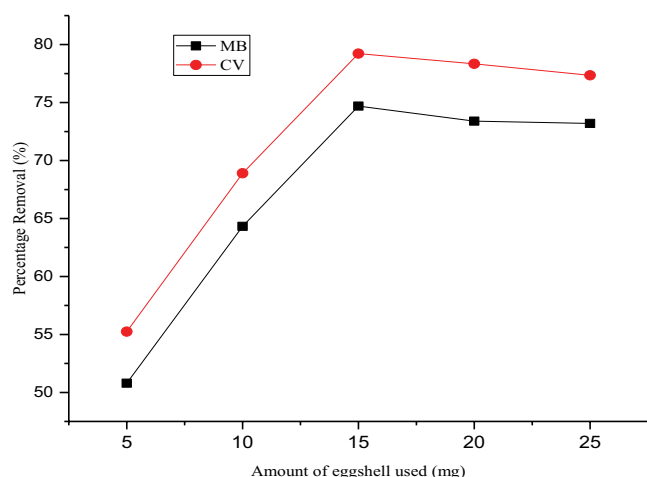


Fig. 7. Effect of eggshell dosage on removal percentage at pH: 5.0, initial pollutant concentration of 500 mg/L, temperature: 35°C, time of 100 and 120 min for MB and CV, respectively.

composed of carboxylic and hydroxyl groups and present at different forms depending on the solution pH. The  $pH_{zpc}$  of the adsorbent has been determined to 4.2 and above this value, the surface charge of the adsorbent is expected to be negatively charged, and cation adsorption occurs. This phenomenon was noticed with the two cationic dyes tested in this study. As the pH of the solution increased, an increase in the adsorption process is due to deprotonation of carboxyl and hydroxyl groups on the adsorbent surface and this resulted in electrostatic attraction that exist between negatively charged sites of the eggshell surface and cationic dye. At higher pH (basic medium), there exists excess of  $OH^-$  of the dyes in solution which eventually resulted in the precipitation of the solution and subsequent low adsorption at higher pH. Thus, the mechanism of both pollutants could be as a result of the electrostatic

attraction between negative surface charged of the eggshell and cationic dyes [4,5,19]. The ionic nature of the two basic dyes (MB and CV) could have played a role in retaining the dye species on the surface of the adsorbents.

#### 3.4. Effect of adsorbent dosage

From the plot of effect of adsorbent dosage on the removal of the dyes shown in Fig. 7, it is evident that the percent removal of the dyes increased as the adsorbent dosage was increased. The percentage removal increased from 51.2% to 73.5% for MB and from 54.1% to 76.7% for CV when the adsorbent dosage was adjusted from 5 to 15 mg. This could be due to the availability of high number of binding sites on the adsorbent surface as provided by the increase in the amount of adsorbent used. Optimum percentage removal of 73.5% and 76.7% was attained at a dosage of 15 mg. The reduction in the removal of the dyes at a higher biomass dosage may be due to agglomeration of the adsorbent as the dosage increases [24–27].

#### 3.5. Kinetics evaluations

The kinetics of the study was explained using pseudo-first-order (PFO), pseudo-second-order (PSO), Elovich and intraparticle diffusion kinetic models as described in Eqs. (4)–(7). Fig. 8 shows the non-linear plots for the models using scientist software and Table 1 shows the parameters calculated from the plots. On comparing the kinetic models based on the correlation coefficients ( $R^2$ ) and the values of %SSE, it was observed that while the pseudo-second-order kinetics model best represented the experimental data for EGP-MB, whereas that of the pseudo-first-order best explained EGP-CV system. The results suggest the mechanism of MB removal by eggshell to be chemisorption, while that of CV removal by eggshell is physisorption [28].

#### 3.6. Isotherm studies

The representations of the isotherm models are given in Fig. 9, and the equilibrium parameters obtained are shown in Table 2. While the adsorption of MB fitted well with the Freundlich isotherm, Langmuir isotherm best described the adsorption parameters of CV as indicated by higher values of the correlation coefficient ( $R^2$ ) when compared with that of the other isotherms. The assumption of the Langmuir isotherm model is such that the homogeneous active site available on the adsorbent structure provides a monolayer adsorption; on the hand, the Freundlich model assumed that the surface of the adsorbent is heterogeneous and therefore provides a non-uniform adsorption process. In addition, the  $R_L$  values for both dyes are less than 1 which indicates that the adsorption of the dyes by eggshell is favorable. The maximum adsorption capacity as obtained from the Langmuir isotherm is 122.510 and 118.610 mg/g for AGP-MG and AGP-CV respectively, whereas, the  $K_f$  parameter from Freundlich isotherm for AGP-MG and AGP-CV are 65.180 and 57.660 (mol/g)(mol/L)<sup>1/n</sup>, respectively indicating that the affinity between the MG dye and the adsorbent surface is superior when compared to CV dye. From D-R analysis, the values of E determined from AGP-MG and



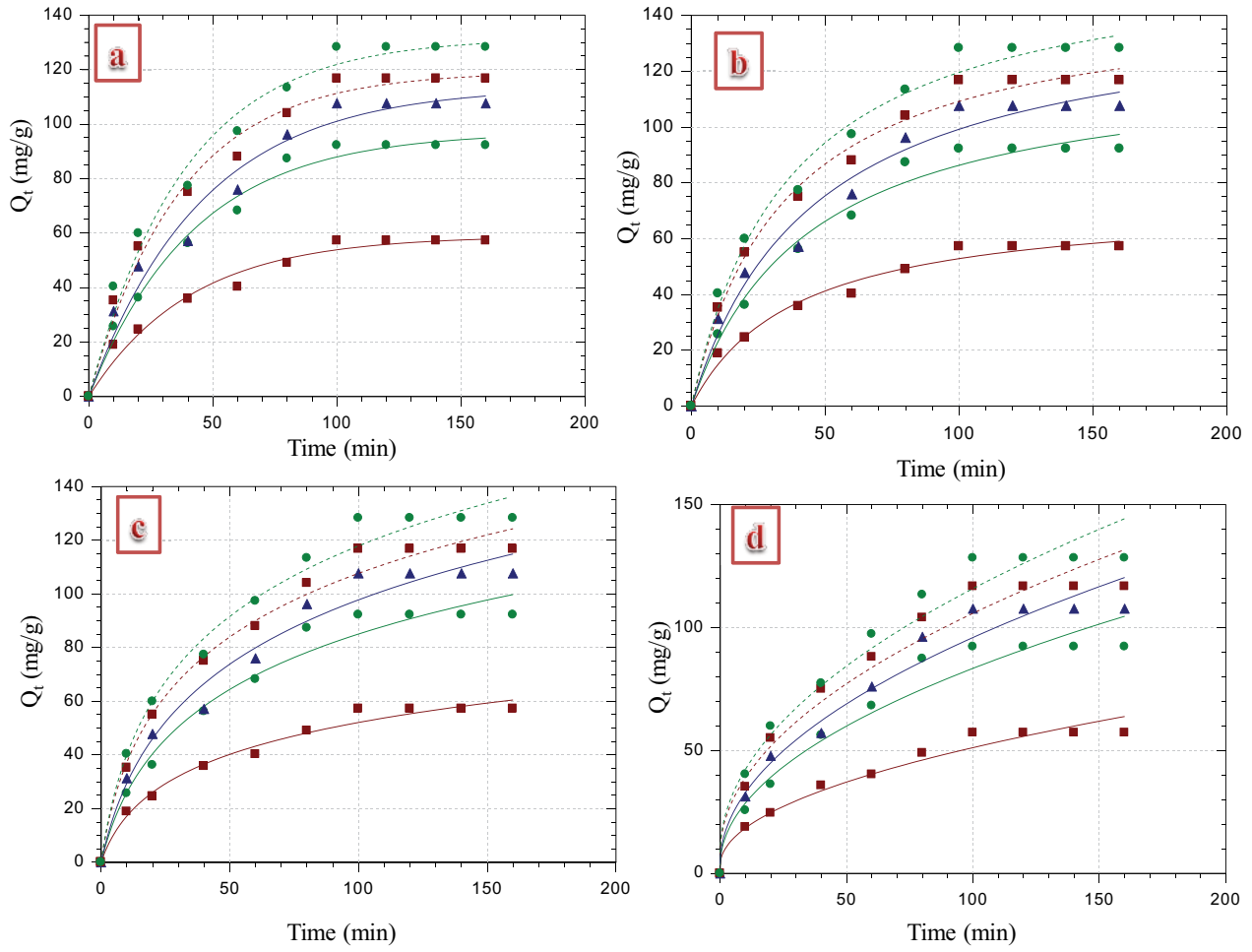


Fig. 8. (a) PFS, (b) PSO, (c) Elovich and (d) intraparticle diffusion kinetic models for the adsorption of CV.

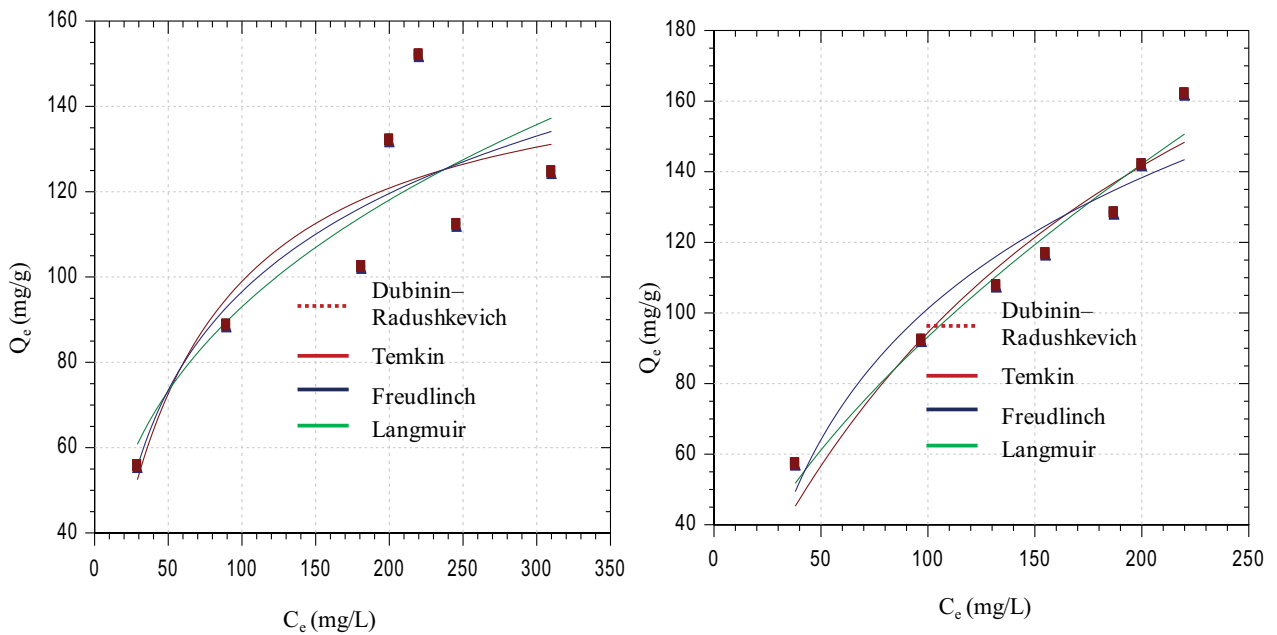


Fig. 9. Isotherm models for the adsorption of MB and CV.

Table 2  
Isotherm parameters for the adsorption of MB and CV onto EGP

Isotherms	Parameter	EGP-MB	EGP-CV
Langmuir	(mg/g)	122.510	118.610
	$b$ (L/mg)	0.029	0.063
	$R_L$	0.064	0.0306
	$R^2$	0.989	0.998
Freundlich	$K_F \times 10^2$ (mol/g)(mol/L) <sup>1/n</sup>	65.180	57.660
	1/n	0.224	0.546
	$R^2$	0.997	0.778
Temkin	$a_T$ (L/mg)	0.338	0.896
	$b_T$	76.568	58.361
	$R^2$	0.894	0.887
Dubinin–Radushkevich	$Q_s$ (mg/g)	102.538	47.200
	$B \times 10^6$ (mol/J) <sup>2</sup>	2.112	4.231
	$E$ (kJ/mol)	0.520	0.835
	$R^2$	0.843	0.915

AGP-CV are 0.520 and 0.835 kJ/mol respectively, and this inferred that the process of adsorption process is physical since  $E < 8$  kJ/mol [29,30].

The maximum adsorption capacities of other studies carried out on the adsorption of MB and CV using different kinds of adsorbent are presented in Table 3. Comparing the adsorption capacity of eggshell powder with those of other adsorbent showed that the adsorbent of the present study is also a promising adsorbent for the removal of dyes from industrial wastewater.

### 3.7. Thermodynamic studies

The impact of temperature on the adsorption process was investigated. The Gibb's free energy change was evaluated using the Eq. (13) [25]:

$$\Delta G^\circ = RT \ln K_c \quad (13)$$

where  $T$  stands for the equilibrium temperature in Kelvin,  $R$  is the ideal gas constant with a value of 8.314 J/mol K and  $K_c$  stands for the thermodynamic equilibrium constant which can be obtained as follows:

$$K_c = \frac{C_a}{C_e} \quad (14)$$

where  $C_a$  denotes the amount of dyes per litre and  $C_e$  is as previously defined in mg/L. The Van't Hoff equation was used to describe the enthalpy change ( $\Delta H^\circ$ ), equilibrium constant and the entropy change ( $\Delta S^\circ$ ) at constant temperature [15]:

$$\ln K_c = \frac{\Delta S^\circ}{R} - \frac{\Delta H^\circ}{RT} \quad (15)$$

The slope and intercept from the plot of  $\ln K_c$  against  $1/T$  (Fig. 10) were used to determine the values of  $\Delta H^\circ$  and  $\Delta S^\circ$  while their values are listed in Table 4. The adsorption

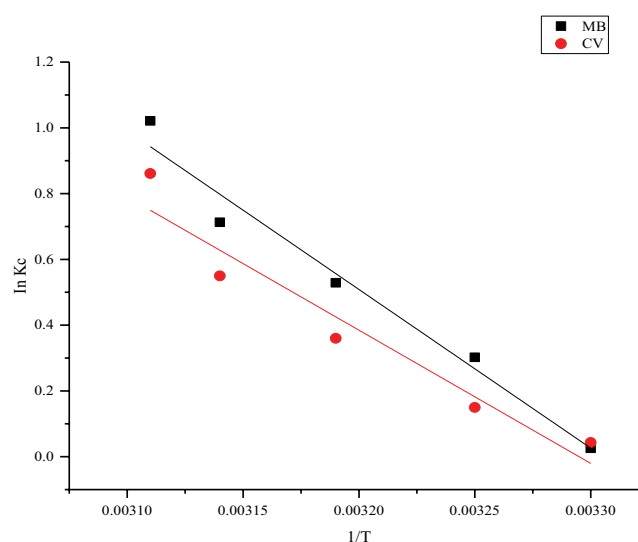


Fig. 10. Plot of thermodynamic parameters.

process is found to be endothermic in nature and random as confirmed from the positive values of  $\Delta H^\circ$  and  $\Delta S^\circ$  respectively. The spontaneity and feasibility of the adsorption process was ascertained from the negative values of  $\Delta G^\circ$  obtained. Also, the values of  $\Delta G^\circ$  were observed to be increasing as temperature increases for the two dyes studied.

## 4. Conclusion

Eggshell powder was investigated for its potency of being an efficient adsorbent for the removal of two cationic dyes from aqueous solution in batch process. The adsorption process was confirmed to be depended on parameters such as contact time, initial dye concentration, pH solution, temperature and adsorbent dosage. The optimum adsorption capacities of 122.510 and 118.610 mg g<sup>-1</sup> were obtained for CV and MB respectively at adsorbent dosage

Table 3

Comparative analysis of adsorption capacities of different adsorbents against that of EGP

Adsorbents	Adsorption capacity (mg/g) Methylene blue	References
Natural clay mineral	100	Omer et al. [9]
Adsorbent-ultrasonic spray	289.85	Song et al. [14]
Magnetite/silica/pectin NPs	178.57	Attallah et al. [19]
Magnetite/pectin NPs	125	Attallah et al. [19]
N-benzyl-O-carboxymethyl chitosan magnetic nanoparticles	223.58	Debrassi et al. [20]
Polymer-modified magnetic nanoparticles	142.9	Ge et al. [21]
Magnetite nanoparticles loaded tea waste	119	Madrakian et al. [31]
Montmorillonite clay modified with iron oxide	71.12	Cottet et al. [32]
Poly(c-glutamic acid) (PGA-MNPs)	78.67	Inbaraj and Chen, [33]
Crystal violet		
Natural clay mineral	330	Omer et al. [9]
Surfactant-modified laterite (SML)	62.6	Ngo et al. [13]
Magnetite/pectin NPs	100	Attallah et al. [19]
Magnetite/silica/pectin NPs	125	Attallah et al. [19]
N-benzyl-O-carboxymethyl chitosan magnetic nanoparticles	248	Debrassi et al. [20]
Polymer-modified magnetic nanoparticles	208.3	Ge et al. [21]
Coal	52.9	Schoonen and Schoonen [22]
Anionic surfactant with silica	40.79	Lin and Lin [23]
Magnetite nanoparticles loaded tea waste	113.69	Madrakian et al. [31]
Coir pith	8.06	Namasivayam et al. [34]

Table 4

Thermodynamic values for the adsorption of MB and CV by EGP

Temp. (K)	MB					CV				
	$K_d$	$\Delta G$ (J/mol)	$\Delta H$ (kJ/mol)	$\Delta S$ (J/mol K)	$R^2$	$K_d$	$\Delta G$ (J/mol)	$\Delta H$ (kJ/mol)	$\Delta S$ (J/mol K)	$R^2$
303	1.016	-38.795				1.026	-40.986			
308	1.094	-80.208				1.353	-74.103			
313	1.521	-91.397	35.471	60.173	0.984	1.697	-106.347	57.172	78.312	0.986
318	2.010	-115.673				2.040	-121.273			
323	2.816	-120.486				2.777	-132.621			

of 1.5 g, contact time of 120 min for MB and 100 min for CV respectively, and pH 5.0. The pseudo-second-order kinetic model best described MB, while pseudo-first-order kinetic model gave good fitting with the adsorption data of CV. It was demonstrated that EGP is a promising and low-cost adsorbent to eliminate cationic dyes of MB and CV in contaminated environment.

### Competing interests

The authors declare that no competing interests exist.

### References

- [1] C. Duran, D. Ozdes, A. Gundogdu, H.B. Senturk, Kinetics and isotherm analysis of basic dyes adsorption onto almond shell (*Prunus dulcis*) as a low cost adsorbent, *J. Chem. Eng. Data*, 56 (2011) 2136–2147.
- [2] E.A. Ofudje, E.F. Sodiya, F. Akinwunmi, A.A. Ogundiran, O.B. Oladeji, O.A. Osideko, Eggshell derived calcium oxide nanoparticles for Toluidine blue removal, *Desal. Water Treat.*, 247 (2022) 294–308.
- [3] K. Vijayaraghavan, S.W. Won, Y.S. Yun, Treatment of complex Remazol dye effluent using sawdust-and coal-based activated carbons, *J. Hazard. Mater.*, 167 (2009) 790–796.
- [4] E.A. Ofudje, E.F. Sodiya, F.H. Ibadin, A.A. Ogundiran, S.O. Alayande, O.A. Osideko, Mechanism of  $\text{Cu}^{2+}$  and reactive yellow 145 dye adsorption onto eggshell waste as low-cost adsorbent, *Chem. Ecol.*, 37 (2021) 268–289.
- [5] A.O. Uzosike, E.A. Ofudje, O.K. Akiode, C.V. Ikenna, A.I. Adeogun, J.O. Akinyele, M.A. Idowu, Magnetic supported activated carbon obtained from walnut shells for bisphenol-A uptake from aqueous solution, *Appl. Water Sci.*, 12 (2022) 201, doi: 10.1007/s13201-022-01724-1.
- [6] A.O. Uzosike, E.A. Ofudje, A.I. Adeogun, J.O. Akinyele, M.A. Idowu, Comparative analysis of bisphenol-A removal efficiency from water: equilibrium, kinetics, thermodynamics and optimization evaluations, *J. Iran. Chem. Soc.*, (2022), doi: 10.1007/s13738-022-02628-2.

- [7] C. Deng, J. Liu, W. Zhou, Y.K. Zhang, K.F. Du, Z.M. Zhao, Fabrication of spherical cellulose/carbon tubes hybrid adsorbent anchored with welan gum polysaccharide and its potential in adsorbing methylene blue, *Chem. Eng. J.*, 200 (2012) 452–458.
- [8] V. Russo, D. Masiello, M. Trifuoggi, M. Di Serio, R. Tesser, Design of an adsorption column for methylene blue abatement over silica: from batch to continuous modelling, *Chem. Eng. J.*, 302 (2016) 287–295.
- [9] S.O. Omer, A.H. Mohammed, H.M.H. Belal, M. Arbi, Adsorption thermodynamics of cationic dyes (methylene blue and crystal violet) to a natural clay mineral from aqueous solution between 293.15 and 323.15 K, *Arabian J. Chem.*, 11 (2018) 615–623.
- [10] L. Vutskits, A. Briner, P. Klauser, E. Gascon, A.G. Dayer, J.Z. Kiss, D.R. Morel, Adverse effects of methylene blue on the central nervous system, *The J. Am. Soc. Anesthesiologists*, 108 (2018) 684–692.
- [11] E.E. Jasper, V.O. Ajibola, J.C. Onwuka, Nonlinear regression analysis of the sorption of crystal violet and methylene blue from aqueous solutions onto an agro-waste derived activated carbon, *Appl. Water Sci.*, 10 (2020) 132, doi: 10.1007/s13201-020-01218-y.
- [12] A. Bondarev, G. Catalina-Gabriela, Adsorptive removal of crystal violet dye from aqueous solutions using natural resource systems, *Desal. Water Treat.*, 264 (2022) 215–223.
- [13] T.M.V. Ngo, T.H. Truong, T.H.L. Nguyen, T.T.A. Duong, T.H. Vu, T.T.T. Nguyen, T.D. Pham, Surface modified laterite soil with an anionic surfactant for the removal of a cationic dye (crystal violet) from an aqueous solution, *Water Air Soil Pollut.*, 231 (2020) 1–15.
- [14] C. Song, Z. Libo, X. Hongying, P. Jinhui, S. Jianhua, L. Chunyang, J. Xin, Z. Qi, Adsorption behavior of methylene blue onto waste derived adsorbent and exhaust gases recycling, *RSC Adv.*, 7 (2017) 27331–27341.
- [15] A.A. Ogundiran, N.A.A. Babarinde, E.A. Ofudje, O.O. Ogundiran, Sequestration of  $\text{Co}^{2+}$ ,  $\text{Zn}^{2+}$  and  $\text{Cd}^{2+}$  by base modified sweet potato leaf: kinetics, equilibrium and thermodynamic studies, *Commun. Phys. Sci.*, 8 (2022) 85–100.
- [16] A.E. Ramirez-Rodriguez, J.L. Reyes-Ledezma, G.M. Chávez-Camarillo, E. Cristiani-Urbina, L. Morales-Barrera, Cyclic biosorption and desorption of acid red 27 onto *Eichhornia crassipes* leaves, *Rev. Mex. Ing. Chim.*, 17 (2018) 1121–1134.
- [17] R. Selvasembian, W. Gwenzi, N. Chaukura, S. Mthembu, Recent advances in the polyurethane-based adsorbents for the decontamination of hazardous wastewater pollutants, *J. Hazard. Mater.*, 417 (2021) 125960, doi: 10.1016/j.jhazmat.2021.125960.
- [18] S. Rangabhashiyam, K. Vijayaraghavan, A.H. Jawad, P. Singh, Sustainable approach of batch and continuous biosorptive systems for praseodymium and thulium ions removal in mono and binary aqueous solutions, *Environ. Technol. Innov.*, 23 (2021) 101581, doi: 10.1016/j.eti.2021.101581.
- [19] A.O. Attallah, M.A. Al-Ghobashy, M. Nebsen, M.Y. Salem, Removal of cationic and anionic dyes from aqueous solution with magnetite/pectin and magnetite/silica/pectin hybrid nanocomposites: kinetic, isotherm and mechanism analysis, *RSC Adv.*, 6 (2016) 11461–11480.
- [20] A. Debrassi, A.F. Corrêa, T. Baccarin, N. Nedelko, A. Slawska-Waniewska, K. Sobczak, P. Dłuzewski, J.M. Greneche, C.A. Rodrigues, Removal of cationic dyes from aqueous solutions using N-benzyl-O-carboxymethyl chitosan magnetic nanoparticles, *Chem. Eng. J.*, 183 (2012) 284–293.
- [21] F. Ge, H. Ye, M-M. Li, B-X. Zhao, Effective removal of cationic dyes from aqueous solution by polymer-modified magnetic nanoparticles, *Chem. Eng. J.*, 198–199 (2012) 11–17.
- [22] M.A. Schoonen, J.M.T. Schoonen, Removal of crystal violet from aqueous solutions using coal, *J. Colloid Interface Sci.*, 422 (2014) 1–8.
- [23] M.C. Lin, K.C. Lin, Interaction between crystal violet and anionic surfactants at silica/water interface using evanescent wave-cavity ring-down absorption spectroscopy, *J. Colloid Interface Sci.*, 379 (2012) 41–47.
- [24] A.A. Ogundiran, N.A.A. Babarinde, E.A. Ofudje, O.O. Ogundiran, Removal of heavy metals from aqueous solutions using modified Irish potato leaf as low cost biosorbent: kinetic and thermodynamic studies, *Pac. J. Sci. Technol.*, 22 (2021) 257–271.
- [25] A.I. Adeogun, A.E. Ofudje, M.A. Idowu, S.A. Ahmed, Kinetic, thermodynamic and isothermal parameters of biosorption of Cr(VI) and Pb(II) ions from aqueous solution by biosorbent prepared from corn cob biomass, *Inorg. Chem. Ind. J.*, 7 (2012) 119–129.
- [26] A.I. Adeogun, E.A. Ofudje, M.A. Idowu, S.O. Kareem, Facile development of nano size calcium hydroxyapatite based ceramic from eggshells: synthesis and characterization, *Waste Biomass Valorization*, 4 (2017), doi: 10.1007/s12649-017-9891-3.
- [27] M.R. Malekbala, S. Hosseini, S.K. Yazdi, S.M. Soltani, M.R. Malekbala, The study of the potential capability of sugar beet pulp on the removal efficiency of two cationic dyes, *Chem. Eng. Res. Des.*, 90 (2012) 704–712.
- [28] A. Alhujaily, H. Yu, X. Zhang, F. Ma, Highly efficient and sustainable spent mushroom waste adsorbent based on surfactant modification for the removal of toxic dyes, *Int. J. Environ. Res. Public Health*, 15 (2018) 1421, doi: 10.3390/ijerph15071421.
- [29] R. Foroutan, S.J. Peighambaroust, S.H. Peighambaroust, M. Pateiro, J.M. Lorenzo, Adsorption of crystal violet dye using activated carbon of lemon wood and activated carbon/ $\text{Fe}_3\text{O}_4$  magnetic nanocomposite from aqueous solutions: a kinetic, equilibrium and thermodynamic study, *Molecules*, 26 (2021) 2241, doi: 10.3390/molecules26082241.
- [30] D. Ozdes, C. Duran, H.B. Senturk, H. Avan, B. Bicer, Kinetics, thermodynamics, and equilibrium evaluation of adsorptive removal of methylene blue onto natural illitic clay mineral, *Desal. Water Treat.*, 52 (2013) 208–218.
- [31] T. Madrakian, A. Afkhami, M. Ahmadi, Adsorption and kinetic studies of seven different organic dyes onto magnetite nanoparticles loaded tea waste and removal of them from wastewater samples, *Spectrochim. Acta, Part A*, 99 (2012) 102–109.
- [32] L. Cottet, C.A.P. Almeida, N. Naidek, M.F. Viante, M.C. Lopes, N.A. Debacher, Adsorption characteristics of montmorillonite clay modified with iron oxide with respect to methylene blue in aqueous media, *Appl. Clay Sci.*, 95 (2014) 25–31.
- [33] B.S. Inbaraj, B.H. Chen, Dye adsorption characteristics of magnetite nanoparticles coated with a biopolymer poly ( $\gamma$ -glutamic acid), *Bioresour. Technol.*, 102 (2011) 8868–8876.
- [34] C. Namasivayam, R. Radhika, S. Suba, Uptake of dyes by a promising locally available agricultural solid waste: coir pith, *Waste Manage.*, 21 (2001) 381–387.